Improvement in the passivation quality of catalytic-chemical-vapor-deposited silicon nitride films on crystalline Si at room temperature

Jun'ichiro Miyaura, and Keisuke Ohdaira*

Japan Advanced Institute of Science and Technology, Nomi, Ishikawa 923-1292, Japan

*E-mail: ohdaira@jaist.ac.jp

We observe an improvement in the passivation quality of silicon nitride (SiN_x) films formed on crystalline silicon wafers by catalytic chemical vapor deposition (Cat-CVD) under the storage at room temperature. Fluorescent light illumination enhances the improvement in the passivation quality of Cat-CVD SiN_x films, although the passivation quality is also improved in the dark. We do not see any change of bonding configurations in the SiN_x films by the storage at room temperature. Capacitance–voltage measurement reveals that an increase in positive charge density in the SiN_x films improves their passivation quality. The improvement in the passivation quality of SiN_x films is observed for SiN_x films deposited at various substrate temperatures, and SiN_x films deposited at higher temperature tends to show more significant improvement in the passivation quality.

Keywords: Silicon nitride, Catalytic chemical vapor deposition, Passivation, Crystalline silicon, Solar cell

1. Introduction

Photovoltaic (PV) technology has become more important owing to an increasing consciousness in global climate change. The development of solar cells with higher efficiency is one of the ways of reducing the cost of PV technology. In crystalline silicon (c-Si) -based solar cells, an interdigitated back-contact (IBC) structure is one promising way to improve the efficiency of c-Si cells because of the absence of shading loss [1–11]. In the IBC cells, high optical transparency, high anti-reflection property, and high passivation ability are particularly required for a surface layer. Silicon nitride (SiN_x) is one of the best materials for the surface layer. This is because it is highly transparent in a wavelength range absorbable in c-Si and has an appropriate refractive index of ~2. SiN_x also has high passivation quality due to hydrogen atoms in it by which Si dangling bonds can be passivated and contains positive charges inducing field-effect passivation particularly for n-type c-Si.

SiN_x films are generally formed by plasma-enhanced chemical vapor deposition (CVD), which can, in principle, induce plasma damage on a c-Si surface. Catalytic CVD (Cat-CVD), also referred to as hot-wire CVD, is a method of depositing thin films by decomposing gas molecules on a heated metal wire through catalytic reaction [12]. Cat-CVD can thus realize plasma-damage-less film deposition and resulting formation of high-quality SiN_x/c-Si interface [13–22]. We have thus far demonstrated the formation of SiN_x passivation films by Cat-CVD showing a surface recombination velocity (SRV) of 5 cm/s [16]. Such a low SRV can be realized after the post-annealing of SiN_x/c-Si samples at 350 °C [16]; however, Si heterojunction back-contact solar cells [1–4], a kind of IBC cells with a-Si/c-Si heterostructures on their back side, requires a low process temperatures of 200 °C or less. It is therefore important to know the passivation quality

of SiN_x films without post-annealing.

In this study, we have observed an improvement in the passivation quality of Cat-CVD SiN_x films under the storage at room temperature. Illumination from fluorescent light for room lighting further enhances the improvement in the passivation quality. The mechanism of the improvement in the passivation quality has also been discussed based on the experimental results of Fourier-transform infrared (FT-IR) spectroscopy, electron spin resonance (ESR), and capacitance–voltage (*C–V*) measurements.

2. Experimental procedures

We used mirror-polished floating-zone-grown n-type c-Si(100) wafers with a resistivity of 1–5 Ωcm and a bulk minority carrier lifetime of >10 ms as substrates. The c-Si wafers were first cleaved into 2×2 cm^2 pieces and native oxide layers on them were removed by dipping in diluted (5%) hydro-fluoric acid (HF) solution. 100-nm-thick SiN_x layers with a refractive index of ~2 were then deposited on both sides of c-Si wafers by Cat-CVD. The deposition of SiN_x films were performed at SiH_4 and NH_3 flow rates of 8 and 150 sccm, respectively, at a pressure of 10 Pa, at substrate and catalyzer temperatures of 100 and 1800 ºC, respectively, for 190 s. This deposition condition has also been utilized in our previous work, by which we obtain SiN_x/c-Si interfaces with an SRV of 5 cm/s after post-annealing at 350 ºC for 30 min [16]. Note that we did not perform the post-annealing of the samples in this study. The thickness and refractive index of the SiN_x films were evaluated by spectroscopic ellipsometry (J. A. Woollam Co., WVASE32) through an analysis using Cauchy model.

We then stored the SiN_x-passivated c-Si samples at room temperature under the following four conditions: in air/under illumination: fluorescent light (~500 lux) or 1-sun

light, in air/in the dark, in vacuum/under the illumination, and in vacuum/in the dark. The quality of SiN_x/Si interfaces was evaluated by measuring the effective minority carrier lifetime (τ_{eff}) of the samples by microwave photoconductivity decay (KOBELCO LTA-1510 EP). A laser pulse with a wavelength of 904 nm and an areal photon density of 5×10^{13} /cm^2 was used for the generation of excess carriers. We measured the τ_{eff} of the samples every 6–24 hours to observe the change of the quality of SiN_x/c-Si interfaces.

We also measured FT-IR spectra of the samples before and after the storage at room temperature to check the variation of bonding configuration in the SiN_x films and H content from Si–H and N–H stretching mode peaks. Bonded hydrogen contents in the SiN_x films were evaluated through the Lanford method [23]. ESR measurement (JEOL JES-FA100) was performed for the SiN_x films before and after the storage at room temperature to evaluate the density of Si dangling bonds in the SiN_x films. The densities of Si dangling bonds in the SiN_x films were quantified by comparing their ESR signals to that of a standard sample with known spin density. The *C–V* curves of SiN_x/c-Si samples were measured on a mercury probe system (MDC 802B) using SiN_x/c-Si/evaporated Al structures.

3. Results and discussion

3.1 Change in τ_{eff} under the storage at room temperature

Figure 1(a) shows the τ_{eff} of c-Si wafers passivated with SiN_x films as a function of storage duration under the four storage conditions, in which fluorescent light illumination was used. The initial τ_{eff} values of the samples were 250–350 μs. One can see monotonic increases in τ_{eff} up to ≥400 μs for all the samples stored in various conditions within the first ~4 days and successive saturations afterwards. To clearly see the degree of τ_{eff}

improvement for individual storage conditions, Fig. 1(a) was replotted as the difference from the initial τ_{eff} values ($\Delta\tau_{eff}$), as shown in Fig. 1(b). Note that the τ_{eff} of the samples stored under fluorescent light shows more significant improvement in τ_{eff}, indicating that the improvement in the passivation quality of SiN_x films can be enhanced by the fluorescent light illumination. We also see no clear impact of atmosphere during the storage (air or vacuum) on the improvement in the τ_{eff} of the samples.

Figure 2 shows the $\Delta\tau_{eff}$ of the c-Si wafers passivated with SiN_x films stored under 1-sun illumination. the $\Delta\tau_{eff}$ of the samples rather decreases under 1-sun illumination, unlike in the case of fluorescent light illumination. The reduction in τ_{eff} may be due to both an increase in an interface state density and a decrease in fixed charge by the illumination, as reported elsewhere [24]. We can thus confirm, from these results, that illumination with proper irradiance is important for the enhancement in the passivation quality of SiN_x/a-Si films.

3.2 Effect of the storage at room temperature on SiN_x film properties

Figure 3 shows the FT-IR spectra of SiN_x films stored in air at room temperature in the dark, under which τ_{eff} is improved by 150 μs as shown in Fig. 1(b). All the peaks in the spectra, originating from Si–N stretching [25], Si–O stretching [26], Si–H stretching [27], and N–H stretching [25] modes, show no change in their intensity. Similar behaviors were also seen in the FT-IR spectra of SiN_x films stored under different conditions (not shown). Based on these results, we can conclude that there are no serious invasions of gas molecules from the atmosphere into SiN_x films and resulting influence on their passivation quality. Figure 4 shows the bonded hydrogen contents obtained from the Si–H and N–H peaks of the FT-IR spectra of SiN_x films stored under various conditions. We

do not see any changes in the hydrogen contents of SiN_x films by the storage at room temperature, independent of the storage conditions. This is also an indication of the absence of the change of bonding configurations in the SiN_x films.

Figure 5 shows the Si dangling bond density of SiN_x films, measured by ESR, as a function of the duration of storage in air under fluorescent light illumination. The Si dangling bond density of SiN_x films first decreases monotonically and then saturates. It should be emphasized that the duration before the saturation of the change of Si dangling bond density is roughly consistent with that of the change of τ_{eff}. This may indicate that the change of Si dangling bond density is related to the improvement in the quality of SiN_x/c-Si interfaces. There are two possibilities for understanding the decrease in the Si dangling bond density of SiN_x films. One is the termination of Si dangling bonds by hydrogen atoms. SiN_x films contain a large number of hydrogen atoms on the order of 10^{22} /cm^3, as shown in Fig. 4, part of which may diffuse inside the SiN_x and make Si–H bonds. This hypothesis does not conflict with the FT-IR results shown in Figs. 3 and 4, since the Si dangling bond density is on the order of 10^{18} /cm^3, which is 4 order of magnitude lower than the hydrogen content in SiN_x and is thus undetectable by FT-IR measurement. The mobile hydrogen atoms may also reach SiN_x/c-Si interfaces and can terminate Si dangling bonds on them. The other possible explanation for the decrease in Si dangling bond density of SiN_x films is the release of electrons from Si defects. ESR can, in principle, detect only unpaired electrons, and ESR signal can thus decrease if Si dangling bonds release electrons. The neutral (with an unpaired electron) and positively charged (with no electron) Si defects back-bonded to three nitrogen atoms are called K^0 and K^+ centers, respectively [28,29]. An increase in the positive charges in SiN_x can also induce an improvement in τ_{eff}, since the positive charges in SiN_x induces downward band

bending in c-Si near the SiN_x/c-Si interface and the density of minority carriers — holes — in the vicinity of the SiN_x/c-Si interface thereby decreases.

To clarify the root cause of the decrease in the Si dangling bond density and the improvement in the SiN_x/Si interfaces, we measured *C–V* curves of SiN_x/c-Si structures before and after the storage at room temperature, the results of which are shown in Fig. 6. The slope of the *C–V* curves, corresponding to the interface state density, does not change significantly by the storage, whereas the curves shift to lower voltage, which indicates an increase in the density of positive charges in SiN_x. We can therefore conclude that the improvement in the quality of SiN_x/c-Si interfaces is not due to the termination of Si dangling bonds on the c-Si surfaces by hydrogen atoms but due to the release of electrons from K^0 centers to c-Si and resulting increase in the density of positive charges and enhanced field-effect passivation. The enhanced improvement in τ_{eff} under fluorescent light illumination might be due to the excitation of electrons in K^0 center sites to the conduction band of SiN_x [25,26], by which electrons can flow into c-Si more easily.

We have finally investigated whether the improvement in the τ_{eff} can be observed for the samples with SiN_x films deposited under different deposition conditions. Figure 7 shows the τ_{eff} of c-Si wafers passivated with SiN_x films deposited at various substrate temperatures of 50–300 °C. One can see improvements in τ_{eff} by storage at room temperature for all the samples. The sample passivated with SiN_x films deposited at higher substrate temperature tends to show more significant improvement in τ_{eff}, and have more duration before the saturation of τ_{eff} improvement. These may be because of the formation of denser SiN_x at higher substrate temperature, which leads to more efficient transition of electrons through SiN_x to c-Si and resulting better field-effect passivation.

One significance obtained this study is that the passivation quality of SiN_x films on

the c-Si solar cells can be changed gradually but largely under storage even at room temperature. The initial performance of c-Si solar cells or modules should thus be evaluated after storage for a few days.

4. Conclusions

We have observed an increase in τ_{eff} with increasing storage duration at room temperature under various storage conditions. In particular, the samples stored under fluorescent light illumination show larger increase in τ_{eff}. The improvement in τ_{eff} can be observed for the samples with SiN_x films deposited at various substrate temperatures. No remarkable changes in the FT-IR spectra of SiN_x films are seen after the storage at room temperature independent of storage conditions. ESR measurement indicates a decrease in the Si dangling bond density of SiN_x films. *C–V* measurements revealed that the cause of the improvement in the passivation quality of SiN_x films is due to an increase in positive charges in SiN_x and resuling enhancement in field-effect passivation.

References

[1] K. Yoshikawa, H. Kawasaki, W. Yoshida, T. Irie, K. Konishi, K. Nakano, T. Uto, D. Adachi, M. Kanematsu, H. Uzu, K. Yamamoto, Silicon heterojunction solar cell with interdigitated back contacts for a photoconversion efficiency over 26%, Nat. Energy **2** (2017) 17032.

[2] K. Yamamoto, K. Yoshikawa, H. Uzu, D. Adachi, High-efficiency heterojunction crystalline Si solar cells, Jpn. J. Appl. Phys. 57 (2018) 08RB20.

[3] K. Masuko, M. Shigematsu, T. Hashiguchi, D. Fujishima, M. Kai, N. Yoshimura, T. Yamaguchi, Y. Ichihashi, T. Mishima, N. Matsubara, T. Yamanishi, T. Takahama, M. Taguchi, E. Maruyama, S. Okamoto, Achievement of more than 25% conversion efficiency with crystalline silicon heterojunction solar cell, IEEE J. Photovoltaics 4 (2014) 1433–1435.

[4] J. Nakamura, N. Asano, T. Hieda, C. Okamoto, H. Katayama, K. Nakamura, Development of heterojunction back contact Si solar cells, IEEE J. Photovoltaics 4 (2014) 1491–1495.

[5] G. Yang, A. Ingenito, O. Isabella, M. Zeman, IBC c-Si solar cells based on ion-implanted poly-silicon passivating contacts, Sol. Energy Mater. Sol. Cells 158 (2016) 84–90.

[6] G. Yang, A. Ingenito, N. van Hameren, O. Isabella, M. Zeman, Design and application of ion-implanted poly-Si passivating contacts for interdigitated back contact c-Si solar cells, Appl. Phys. Lett. 108 (2016) 033903.

[7] D. L. Young, W. Nemeth, V. LaSalvia, R. Reedy, S. Essig, N. Bateman, P. Stradins, Interdigitated back passivated contact (IBPC) solar cells formed by ion implantation, IEEE J. Photovoltaics 6 (2016) 41–47.

[8] D. D. Smith, P. Cousins, S. Westerberg, R. De Jesus-Tabajonda, G. Aniero, Y. -C. Shen, Toward the practical limits of silicon solar cells, IEEE J. Photovoltaics 4 (2014) 1465–1469.

[9] T. Rahman , H. T. Nguyen , A. Tarazona, J. Shi, Y.-J. Han, E. Franklin, D. Macdonald, S. A. Boden, Characterization of epitaxial heavily doped silicon regions formed by hot-wire chemical vapor deposition using micro-Raman and microphotoluminescence spectroscopy, IEEE J. Photovoltaics 8 (2018) 813–819.

[10] T. Rahman, A. Nawabjan, A. Tarazona, D. M. Bagnall, S. A. Boden, Junction formation with hot-wire CVD and TCAD model of an epitaxial back-contact solar cell, IEEE J. Photovoltaics 6 (2016) 1396–1402.

[11] E. Khorani, T. Scheul, A. Tarazona, T. Rahman, S. A. Boden, Optimisation of ex-situ annealing process for epitaxial silicon emitters via hot wire CVD, Proc. 14th Photovoltaic Sci. Appl. Technol. Conf., London, United Kingdom, 2018.

[12] H. Matsumura, Catalytic chemical vapor deposition (CTC–CVD) method producing high quality hydrogenated amorphous silicon, Jpn. J. Appl. Phys. 25 (1986) L949–L951.

[13] K. Koyama, K. Ohdaira, H. Matsumura, Extremely low surface recombination velocities on crystalline silicon wafers realized by catalytic chemical vapor deposited SiN_x/a-Si stacked passivation layers, Appl. Phys. Lett. 97 (2010) 082108.

[14] K. Koyama, K. Ohdaira, H. Matsumura, Excellent passivation effect of Cat-CVD SiN_x/i-a-Si stack films on Si substrates, Thin Solid Films 519 (2011) 4473–4475.

[15] Trinh Cham Thi, K. Koyama, K. Ohdaira, H. Matsumura, Passivation characteristics of SiN_x/a-Si and SiN_x/Si-rich SiN_x stacked layers on crystalline silicon, Sol. Energy Mater. Sol. Cells 100 (2012) 169–173.

[16] Trinh Cham Thi, K. Koyama, K. Ohdaira, H. Matsumura, Passivation quality of a stoichiometric SiN_x single passivation layer on crystalline silicon prepared by Cat-CVD and successive annealing, Jpn. J. Appl. Phys. 53 (2014) 022301.

[17] Trinh Cham Thi, K. Koyama, K. Ohdaira, H. Matsumura, Drastic reduction in the surface recombination velocity of crystalline silicon passivated with Cat-CVD SiN_x films by introducing phosphorous Cat-doped layer, J. Appl. Phys. 116 (2014) 044510.

[18] Trinh Cham Thi, K. Koyama, K. Ohdaira, H. Matsumura, Effect of hydrogen on passivation quality of SiN_x/Si-rich SiN_x stacked layers deposited by catalytic chemical vapor deposition on c-Si wafers, Thin Solid Films 575 (2015) 60–63.

[19] K. Ohdaira, Trinh Thi Cham, H. Matsumura, Passivation of textured crystalline silicon surfaces by catalytic CVD silicon nitride films and catalytic phosphorus doping, Jpn. J. Appl. Phys. 56 (2017) 102301.

[20] Trinh Cham Thi, K. Koyama, K. Ohdaira, H. Matsumura, Defect termination on c-Si surfaces by hydrogen for improvement in the passivation quality of Cat-CVD SiN_x and SiN_x/P Cat-doped layers, Jpn. J. Appl. Phys. 55 (2016) 02BF09.

[21] C. T. Nguyen, K. Koyama, S. Terashima, C. Okamoto, S. Sugiyama, K. Ohdaira, H. Matsumura, Novel chemical cleaning of textured crystalline silicon for realizing surface recombination velocity <0.2 cm/s using passivation Cat-CVD SiN_x/a-Si stacked layers, Jpn. J. Appl. Phys. 56 (2017) 056502.

[22] H. T. C. Tu, K. Koyama, C. T. Nguyen, K. Ohdaira, H. Matsumura, High-quality surface passivation of c-Si with chemical resistance and optical transparency by using Cat-CVD SiN_x double layers and an ultra-thin SiO_x film, Jpn. J. Appl. Phys. 57 (2018) 08RB17.

[23] W. A. Lanford, M. J. Rand, The hydrogen content of plasma-deposited silicon nitride,

J. Appl. Phys. 49 (1978) 2473–2477.

[24] Z. R. Chowdhury, N. P. Kherani, Light-induced degradation of native silicon oxide–silicon nitride bilayer passivated silicon, Appl. Phys. Lett. 107 (2015) 151602

[25] E. A. Taft, Characterization of silicon nitride films, J. Electrochem. Soc. 118 (1971) 1341–1346.

[26] F. L. Galeener, G. Lucovsky, Longitudinal Optical Vibrations in Glasses: GeO_2 and SiO_2, Phys. Rev. Lett. 37 (1976) 1474–1478.

[27] G. Lucovsky, R. J. Nemanich, J. C. Knights, Structural interpretation of the vibrational spectra of a-Si: H alloys, Phys. Rev. B 19 (1979) 2064–2073.

[28] J. Robertson, M. J. Powell, Gap states in silicon nitride, Appl. Phys. Lett. 44 (1984) 415.

[29] S. A. Cabañas-Tay, L. Palacios-Huerta, J. A. Luna-López, M. Aceves-Mijares, S. Alcántara-Iniesta, S. A. Pérez-García, A. Morales-Sánchez, Analysis of the luminescent centers in silicon rich silicon nitride light-emitting capacitors, Semicond. Sci. Technol. 30 (2015) 065009.

Figure Captions

Fig. 1 (a) τ_{eff} and (b) $\Delta\tau_{eff}$ of c-Si wafers passivated with SiN_x passivation films as a function of storage duration under the four storage conditions.

Fig. 2 $\Delta\tau_{eff}$ of c-Si wafers passivated with SiN_x films as a function of storage duration under 1-sun illumination. $\Delta\tau_{eff}$ of the samples stored in the dark is also shown for comparison.

Fig. 3 FT-IR spectra of SiN_x films stored in air in the dark measured at various storage durations.

Fig. 4 Hydrogen contents of SiN_x films stored (a) in air and (b) in vacuum as a function of storage duration.

Fig. 5 Si dangling bond density of SiN_x films stored in air under fluorescent light illumination as a function of storage duration. The solid line is a guide for the eye.

Fig. 6 *C–V* curves of SiN_x/c-Si structures before and after the storage at room temperature for 24 hours in air under fluorescent light illumination.

Fig. 7 τ_{eff} of c-Si wafers passivated with SiN_x films deposited at various substrate temperatures as a function of the duration of storage in air under fluorescent light illumination.

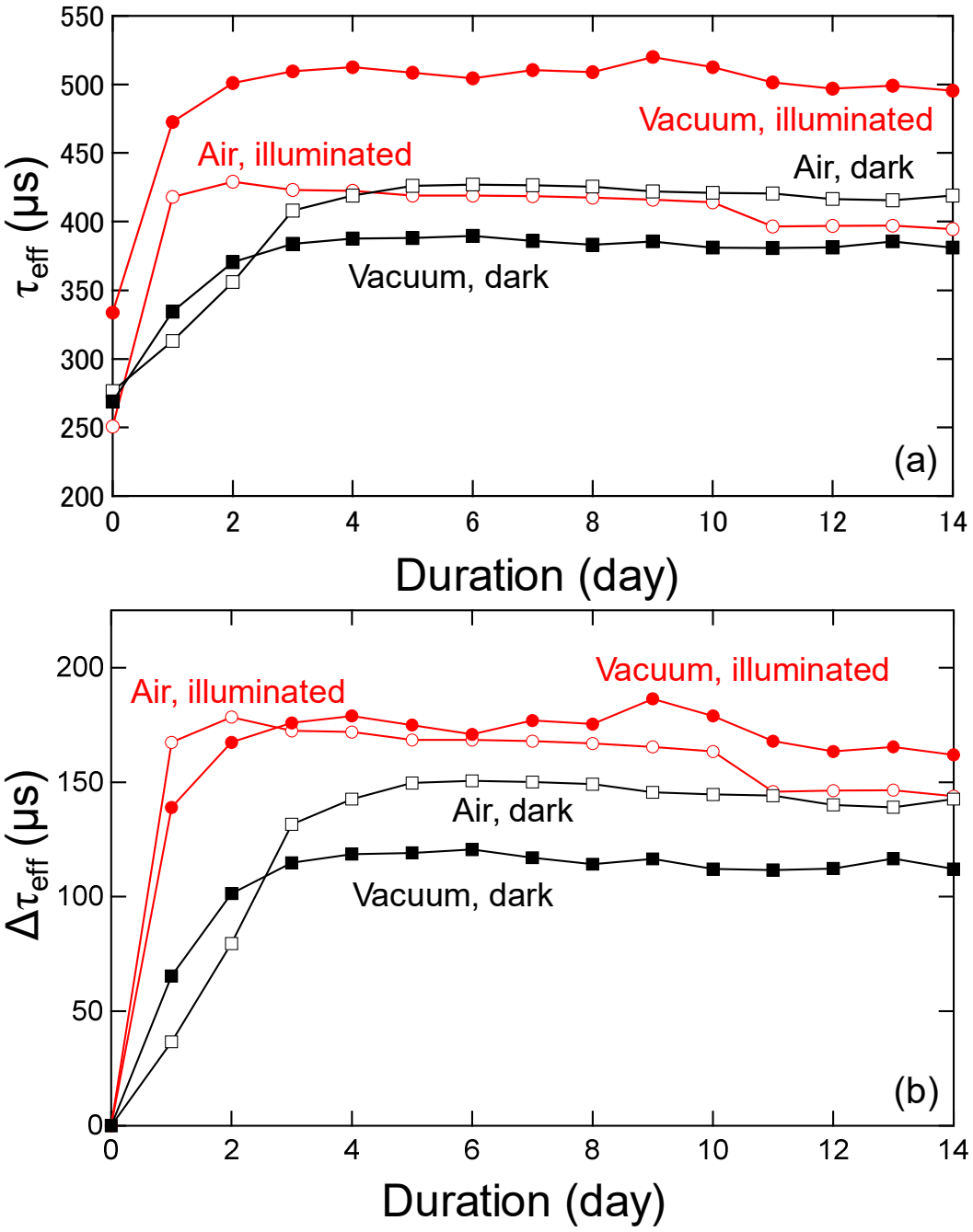
550
500
450
400
350
300
250
200
τ_{eff} (μs)
Vacuum, illuminated
Air, illuminated
Air, dark
Vacuum, dark
(a)
0
2
4
6
8
10
12
14
Duration (day)
200
150
100
50
0
$\Delta\tau_{eff}$ (μs)
Air, illuminated
Vacuum, illuminated
Air, dark
Vacuum, dark
(b)
0
2
4
6
8
10
12
14
Duration (day)

Fig. 1

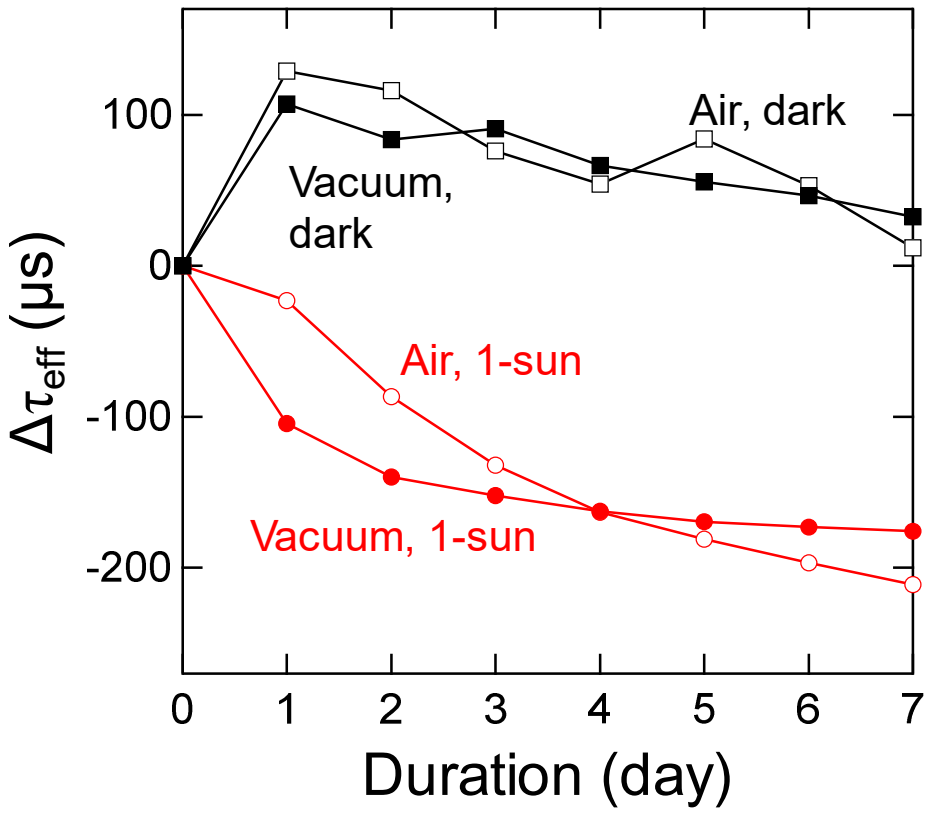
100
0
-100
-200
$\Delta\tau_{eff}$ (μs)
Air, dark
Vacuum,
dark
Air, 1-sun
Vacuum, 1-sun
0
1
2
3
4
5
6
7
Duration (day)

Fig. 2

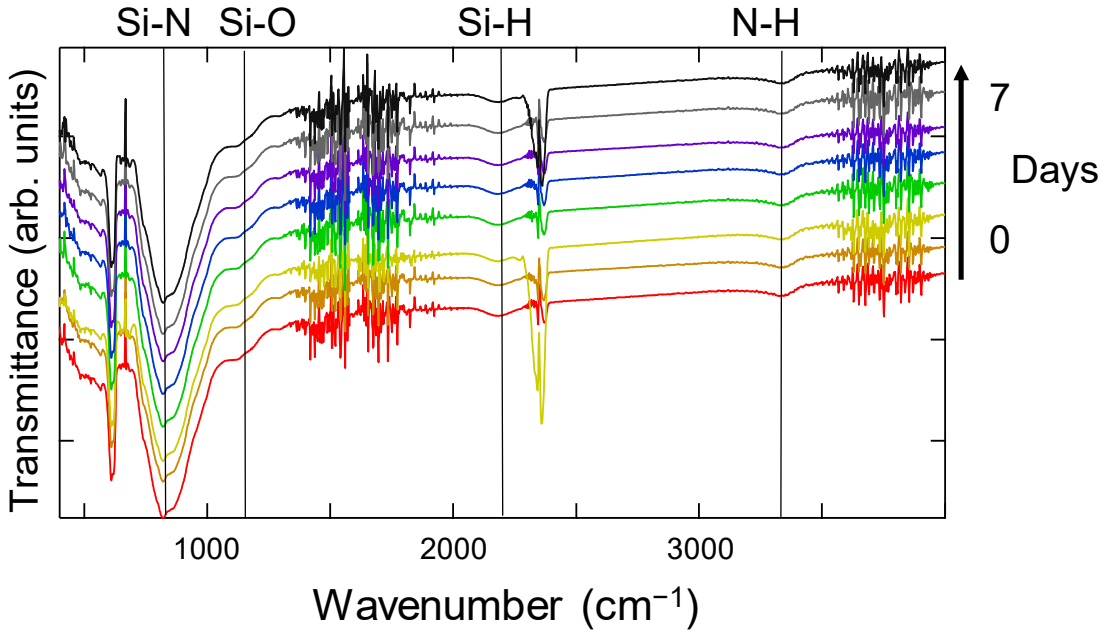
Si-N
Si-O
Si-H
N-H
Transmittance (arb. units)
7
Days
0
1000
2000
3000
Wavenumber (cm^{-1})

Fig.3

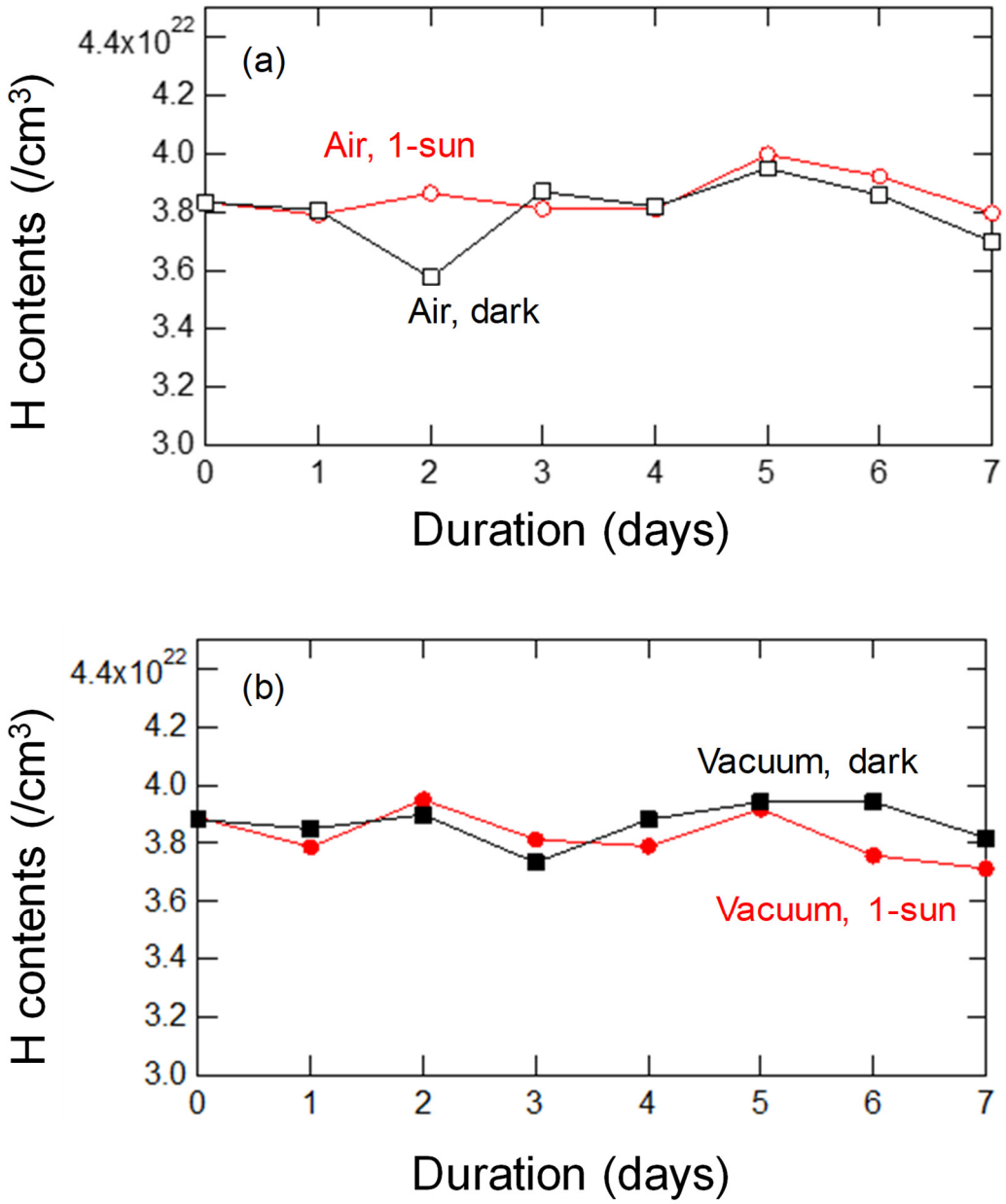
(a)
Air, 1-sun
Air, dark
H contents (/cm3)
4.4x1022
4.2
4.0
3.8
3.6
3.4
3.2
3.0
0
1
2
3
4
5
6
7
Duration (days)
(b)
Vacuum, dark
Vacuum, 1-sun
H contents (/cm3)
4.4x1022
4.2
4.0
3.8
3.6
3.4
3.2
3.0
0
1
2
3
4
5
6
7
Duration (days)

Fig. 4

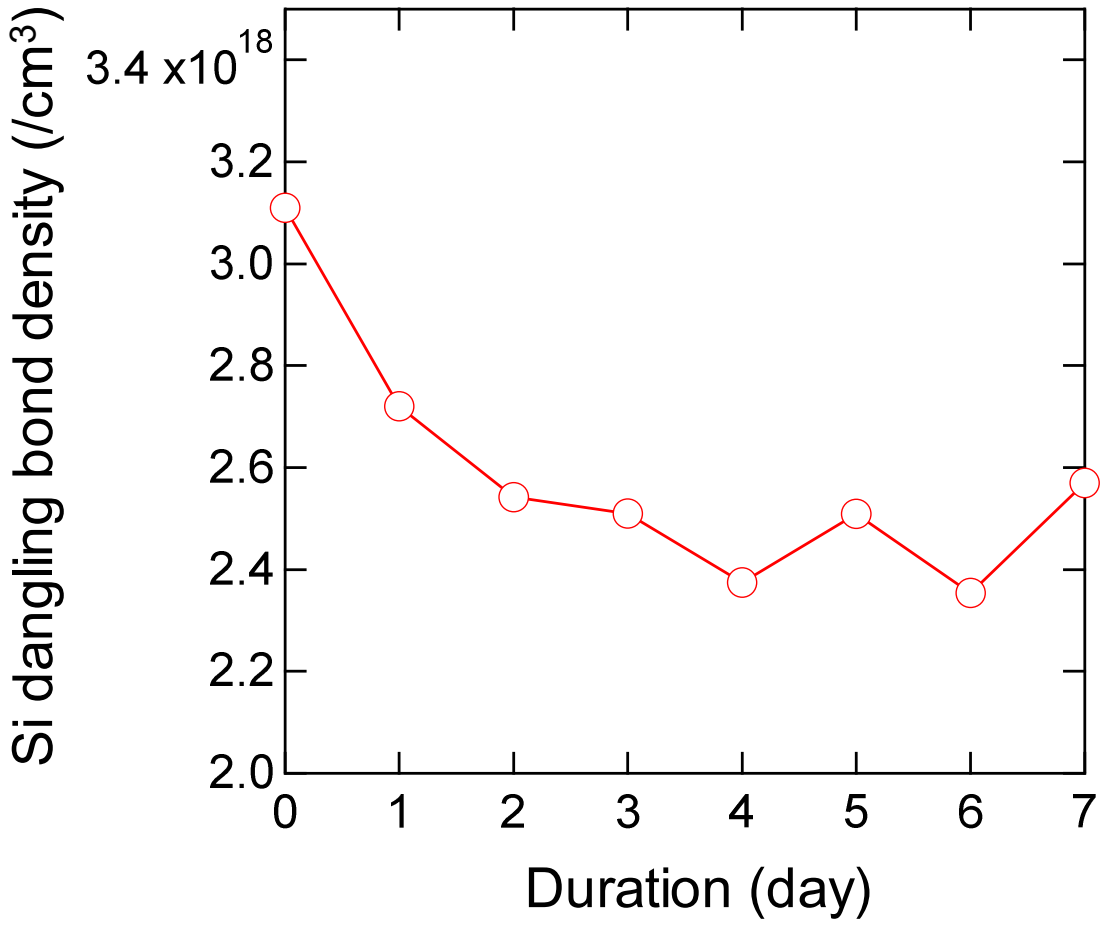
Si dangling bond density (/cm3)
3.4 x1018
3.2
3.0
2.8
2.6
2.4
2.2
2.0
0
1
2
3
4
5
6
7
Duration (day)

Fig. 5

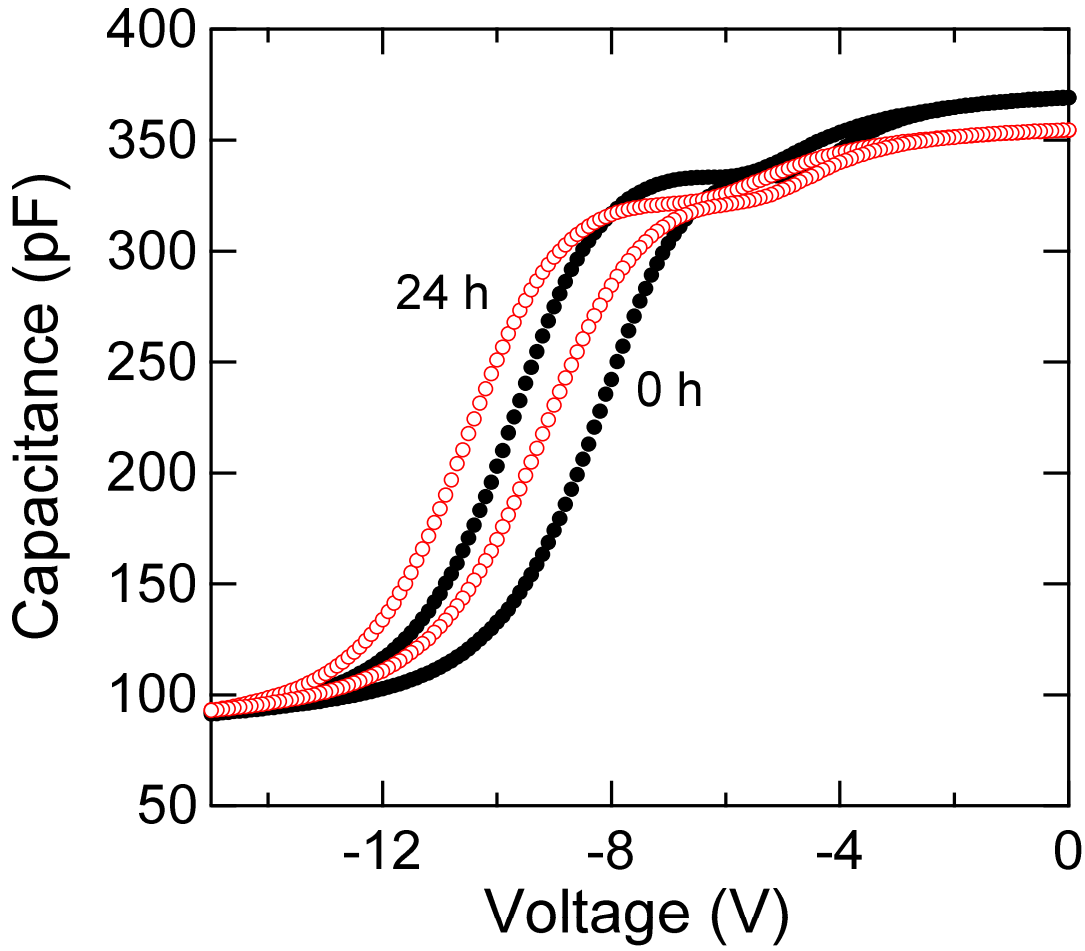
400
350
300
250
200
150
100
50
Capacitance (pF)
24 h
0 h
-12
-8
-4
0
Voltage (V)

Fig. 6

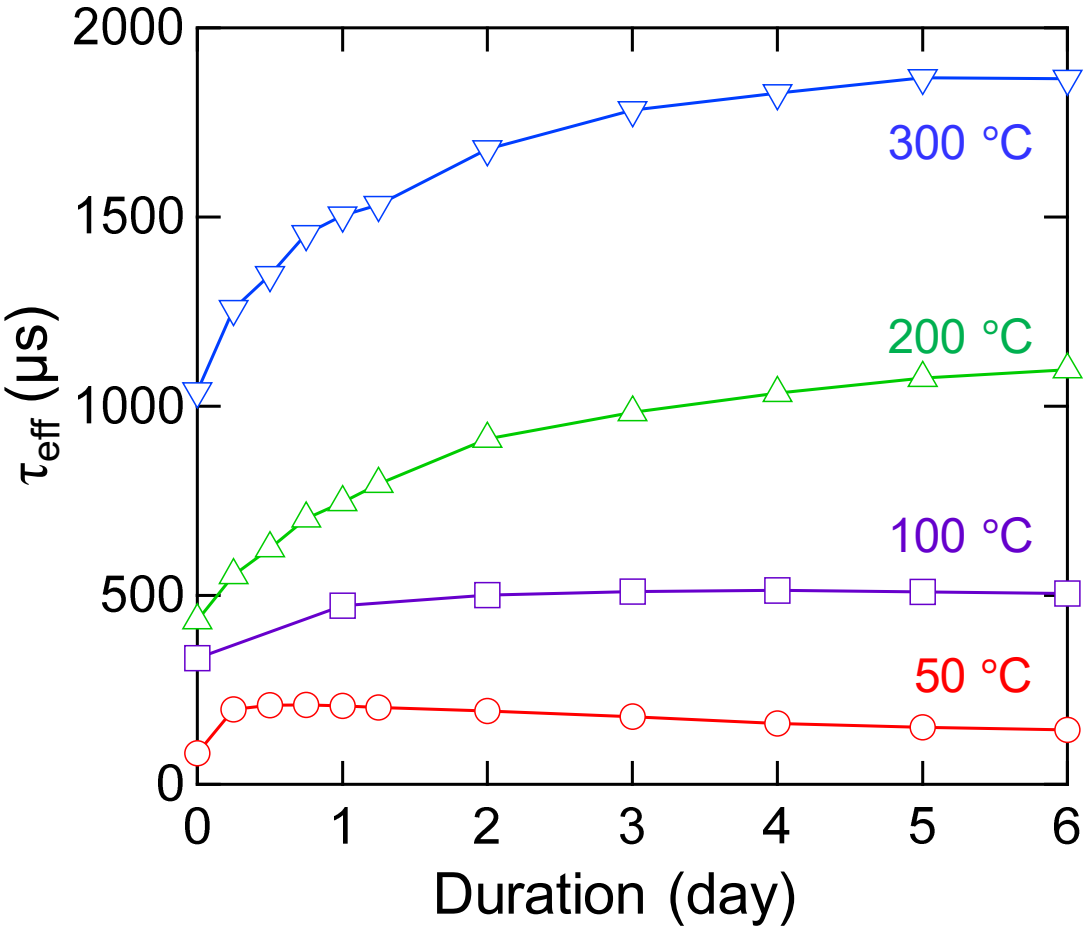
2000
1500
1000
500
0
τ_{eff} (μs)
300 °C
200 °C
100 °C
50 °C
0
1
2
3
4
5
6
Duration (day)

Fig. 7